[12]N. Bohr, K. Dan. Vidensk. Selsk., Mat. Fys. Medd. 18, No. 8 (1948).
[13]J. Neufeld and R. H. Ritchie, Phys. Rev. 98, 1632 (1955).
[14]J. Neufeld and R. H. Ritchie, Phys. Rev. 99, 1125 (1955).
[15]J. Hubbard, Proc. Phys. Soc., London, Sect. A 68, 976 (1955).
[16]M. G. Calkin and P. J. Nicholson, Rev. Mod. Phys. 39, 361 (1967).
[17]R. K. Nesbet and J. F. Ziegler, unpublished result.
[18]J. D. Jackson, *Classical Electrodynamics* (Wiley, New York, 1975).
[19]M. Abramowitz and I. A. Stegun, *Handbook of Mathematical Functions* (Dover, New York, 1965).
[20]V. N. Neelavathi, R. H. Ritchie, and W. Brandt, Phys. Rev. Lett. 33, 302 (1974).
[21]W. Brandt, A. Ratkowski, and R. H. Ritchie, Phys. Rev. Lett. 33, 1325 (1974).
[22]W. Brandt and R. H. Ritchie, Nucl. Instrum. Methods 132, 43 (1976).
[23]W. Brandt, R. Laubert, and A. Ratkowski, Nucl. Instrum. Methods 132, 57 (1976).
[24]R. H. Ritchie, W. Brandt, and P. M. Echenique, Phys. Rev. B 14, 4808 (1976).
[25]D. S. Gemmell, J. Remillieux, J.-C. Poizat, M. J. Gaillard, R. E. Holland, and Z. Vager, Phys. Rev. Lett. 34, 1420 (1975).
[26]Z. Vager, D. S. Gemmell, and B. J. Zabransky, Phys. Rev. A 14, 638 (1976).
[27]D. S. Gemmell, J. Remillieux, J.-C. Poizat, M. J. Gaillard, R. E. Holland, and Z. Vager, Nucl. Instrum. Methods 132, 61 (1976).
[28]J. W. Tape, W. M. Gibson, J. Remillieux, R. Laubert, and H. E. Wegner, Nucl. Instrum. Methods 132, 75 (1976).
[29]Z. Vager and D. S. Gemmell, Phys. Rev. Lett. 37, 1352 (1976).
[30]N. R. Arista and V. H. Ponce, J. Phys. C 8, L188 (1975).
[31]S. Chandrasekhar, Rev. Mod. Phys. 15, 1 (1943).
[32]A proper treatment necessarily involves integration of the interference term over the relevant pair correlation function. This treatment is lengthy and will be the subject of future publication. Reliable estimates, however, are made based on the physically transparent model given here.
[33]B. J. Eastlund, Nucl. Fusion 11, 15 (1971).
[34]It is noted that the derivation of the instability growth rate breaks down in this limit since the standard derivation makes the assumption that $\delta/\omega_b \ll 1$.
[35]I. F. Kharchenko, Ya. B. Fainberg, R. M. Nikolaev, E. A. Kornilov, E. I. Lutsenko, and N. S. Pedenko, Atomic Energy Commission Report No. AEC-Tr-4181, 1960 (unpublished).
[36]D. A. Hammer and K. Papadopoulos, Nucl. Fusion 15, 977 (1975).
[37]G. I. Budker, At. Energ. 5, 9 (1956).
[38]V. I. Veksler, At. Energ. 2, 427 (1957) [Sov. J. Atomic Energy 2, 525 (1957)].
[39]W. O. Doggett and W. H. Bennett, Bull. Amer. Phys. Soc. 14, 1048 (1969), and 15, 641, (1970); W. O. Doggett, Bull. Amer. Phys. Soc. 15, 1347 (1970).
[40]H. Hirakawa, Phys. Fluids 18, 1140 (1975).

High-Density Discharges in the Alcator Tokamak

M. Gaudreau, A. Gondhalekar, M. H. Hughes,[a] D. Overskei, D. S. Pappas, R. R. Parker, S. M. Wolfe, E. Apgar, H. I. Helava, I. H. Hutchinson, E. S. Marmar, and K. Molvig
Francis Bitter National Magnet Laboratory and Plasma Fusion Center, Massachusetts Institute of Technology Cambridge, Massachusetts 02139
(Received 31 August 1977)

Peak plasma densities in excess of 10^{15} cm^{-3} have been obtained in the Alcator tokamak with $60 \leq B_T < 85$ kG. The highest average density so far achieved is $\bar{n}_e = 6\times10^{14}$ cm^{-3}; the corresponding $n_0\tau_E = 2\times10^{13}$ cm^{-3} s. These ultrahigh-density discharges exhibit (i) nearly complete energy equilibration between electrons and ions, (ii) severe attenuation of energetic-neutral-particle fluxes, (iii) a minor role of impurities, and (iv) energy-confinement properties consistent with neoclassical estimates.

The unique combination of high toroidal field, current, and Ohmic power density, together with clean vacuum and wall conditions in the Alcator tokamak has previously enabled discharges with densities ranging from 5×10^{12} cm^{-3} to 5×10^{14} cm^{-3} to be produced. These discharges had particular significance because they made possible a comprehensive study of confinement properties as a function of density, n, which showed that the global energy-confinement time, τ_E, increases roughly in proportion to the density.[1-4] Hence the Lawson parameter, $n_0\tau_E$ (n_0 is the central density), increases in proportion to n^2, and values of $n_0\tau_E$ up to 1×10^{13} cm^{-3} s have been reported.

Recent improvements in the operation of Alcator have permitted further increases in density, and central densities in excess of 10^{15} cm^{-3} have now been produced at toroidal fields between 60

and 85 kG. The following observations have been made in these ultrahigh-density discharges: (1) Nearly complete thermal equilibration between electrons and ions is achieved. (2) The charge-exchanged neutral flux with energy above 200 eV is decreased by a factor of about 100 relative to the corresponding flux at $n = 10^{14}$ cm^{-3}; the potential for sputtering of the vacuum wall by neutral particles is thus greatly reduced. The calculated flux of heavy impurities into the plasma from the stainless-steel wall due to physical sputtering thereby decreases by a factor of 50. (3) Impurities continue to play a minor role in determining the plasma resistivity and central power balance. (4) τ_E continues to increase with $\bar{n}$, and values of $n_0\tau_E$ of 2×10^{13} cm^{-3} s have now been achieved. (5) Values of the total energy-confinement time and poloidal beta, β_θ, are consistent with neoclassical estimates.

Equilibrium is first established in a low-density plasma ($\bar{n}\approx 3\times10^{13}$ cm^{-3}); approximately 10 ms after the initiation of the discharge, cold neutral gas is injected into the chamber through a programmed fast valve, bringing the density to its final value. Two conditions facilitate production of stable high-density discharges: (1) high Ohmic-power density[5]; and (2) a slight positive slope in the plasma current, i.e., $dI_p/dt > 0$, during the density rise.

Typical values of the principal discharge parameters are listed in Table I. Thomson scattering of ruby-laser light at four radial positions yield spatial profiles of electron temperature and relative density. A 119-μm modulated interferometer[6] is used to calibrate the Thomson scattering measurements and thereby determine absolute density. The central current density, j_0, and safety factor q_0, are obtained in the usual way from the electron temperature profile, using the assumption of Spitzer resistivity, $\eta \propto T_e^{-3/2}$. The resistive-loop voltage is determined from the measured total loop voltage, corrected for the time variation of poloidal flux between the plasma and voltage loops, where the mutual inductance involved has been measured directly. For the discharge tabulated in Table I, the average Ohmic power density is $\cong 4$ W cm^{-3} and the peak power density in the plasma center is about 24 W/cm^3. Under these circumstances, a maximum rate of line-averaged plasma density increase of 10^{13}/cm^3 ms can be sustained without causing disruption. In this case nearly 20% of the available Ohmic power is consumed by the density rise.

The ion temperature is determined by measuring the rate of thermonuclear-neutron emission. Assuming that the ion temperature and density profiles are identical to the corresponding measured electron profiles, a rate of thermonuclear-neutron emission is calculated with the central ion temperature as a free parameter. By comparing the calculated neutron emission rate with that experimentally observed, the central ion temperature is deduced. Figure 1 shows a com-

TABLE I. Typical high-density–discharge parameters in D_2. The first two columns list experimentally measured parameters for two magnetic fields. The safety factor q, resistivity η, confinement time τ_E, and poloidal beta β_θ are determined from the Thomson data. The third column lists the results from the neoclassical code where the toroidal field B_T, plasma current I_p, and the average $\bar{n}_e$, are given.

	Typical discharge parameters in D_2		Neoclassical code results
B_T (kG)	60	82	80
I_p (kA)	160	160	160
V_R (V)	3.0	2.7	2.6
$\bar{n}_e$ (10^{14} cm^{-3})	5.3	5.0	4.9
n_0 (10^{14} cm^{-3})	10	11	8.1
T_{e0} (eV)	656	886	772
T_{i0} (eV)	575	...	691
q_0	0.8	0.8	1.4
q ($r = 9$ cm)	2.9	3.9	3.0 ($r = 8$ cm)
$\langle\eta/\eta_{cl}\rangle$	0.9	0.95	1.0
τ_E (ms)	16.6	18.4	20.0
β_θ	1.2	1.2	1.3

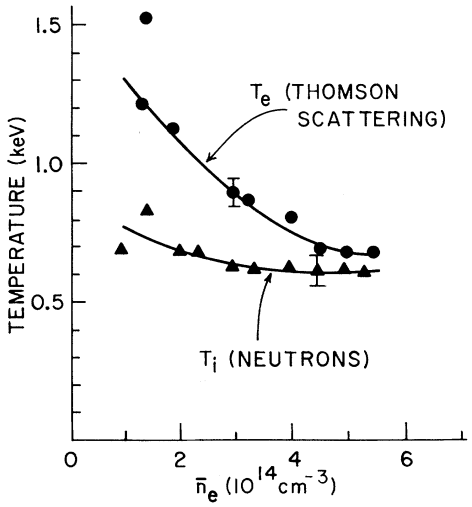

FIG. 1. Central electron and ion temperatures determined by Thomson scattering and neutron emission, respectively, vs line-average electron density. Uncertainty in each of these measurements is within ±10%. These measurements were made at $I_P \approx 160$ kA and $B_T = 60$ kG.

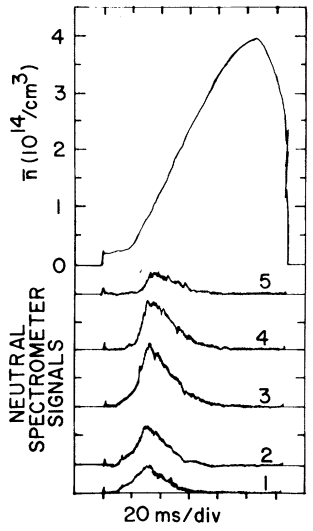

FIG. 2. Cutoff of energetic neutral flux during a high-density discharge. The top trace is line-average electron density obtained from the 119-μm laser. The lower traces are unnormalized signals from the five analyzer channels: (1) 500 eV, (2) 685 eV, (3) 974 eV, (4) 1321 eV, and (5) 1947 eV. Note the decrease in the flux for average densities in excess of 1×10^{14} cm^{-3}.

parison between peak ion temperatures and the corresponding peak electron temperatures measured by Thomson scattering.

We have also determined ion temperature by measuring the energy spectrum of the neutral outflux. This method agrees within 10% of the value measured by the neutron technique over the density range $(1-3)\times10^{14}$ cm^{-3}. Direct measurement of the peak ion temperature by energy analysis of charge-exchanged neutrals is not possible at higher densities because of the opacity of the plasma to neutrals. For example, at an energy of 1 keV and $n=10^{15}$ cm^{-3}, a neutral hydrogen atom has a mean free path of 0.4 cm compared to the plasma radius of 10 cm. Thus, the outgoing flux of energetic neutrals is severely attenuated, dropping nearly two orders of magnitude as the plasma density exceeds a critical value of approximately $\bar{n}\sim1.5\times10^{14}$ cm^{-3} as illustrated in Fig. 2. The detection system has a low-energy cutoff at about 200 eV. Calculations also show that above densities of 3×10^{14} cm^{-3} the neutral outflux does not have an energy spectrum characteristic of the central ion distribution function, the deviation being such as to give an underestimate of the central ion temperature T_{i0}.[7,8]

In addition to the shielding effect, the shortening of the neutral mean free path leads to a substantial decrease of the central neutral density. We believe this effect is initially responsible for the drop in the outgoing flux, since the density at which this occurs is independent of energy. The observations are in qualitative agreement with the results of the theory of the neutral-gas component in opaque regimes[7,8] and also with numerical simulations.[9] These calculations show that the central neutral density is insufficient by more than an order of magnitude to account for the observed rate of plasma density rise. This, in agreement with the charge-exchange data at lower densities, implies that the central density rise is caused by an inward flow of plasma, rather than by local ionization of neutral gas.

Extensive measurements of the soft-x-ray flux and impurity emission in the vacuum ultraviolet have been made. Typical values of $Z_{\rm eff}$ of 0.9 ±0.5 and 1.2±0.2 have been deduced from the soft-x-ray bremsstrahlung[10] and ultraviolet impurity emission,[11] respectively, consistent with the observed $\langle\eta/\eta_s\rangle\approx1$. Power radiated by line radiation from light impurities and hydrogen near the edge of the plasma is about 7% and 2%, respectively, of the total Ohmic power input. The power radiated from the principal heavy impurity, molybdenum, is less than 2% of the Ohmic input.

The neoclassical transport theory of tokamaks predicts that the energy-confinement time should

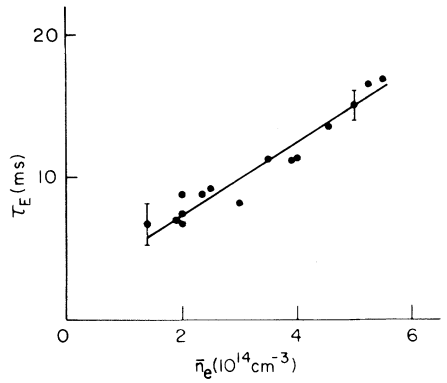

FIG. 3. Global energy-confinement times vs average density. Data were obtained from $B_T = 60$ kG, $I_p = 155$–180 kA discharges using independently obtained ion and electron temperatures. Confinement times for largest densities agree with neoclassical predications. Typical error bars are shown.

decrease as the collision frequency increases. In Alcator, however, an increase in the global energy-confinement time with density has been consistently observed. We have investigated the dependence of τ_E on $\bar{n}$ in these ultrahigh-density regimes, keeping the toroidal field and plasma current constant; measurements made at different values of B_T and I_p have also indicated a weak dependence of τ_E on q. The data, as shown in Fig. 3, is reasonably well represented by the simple scaling $\tau_E \simeq 1.7 q^{1/2} \bar{n}_{14}$ ms, which has been found previously.[3] It should be emphasized that such scaling laws only represent trends in the data and cannot take into account the complicated physical phenomena which occur over the total range of all parameters. For operating conditions as those for data in Fig. 3, at the highest densities the peak temperature drops and the loop voltage increases. This is suggestive of a decrease of τ_E/n in the central region of the plasma. Detailed measurements have indeed shown such behavior. A full discussion of the energy balance of the central core of the plasma, demonstrating behavior dominated by neoclassical ion heat conductivity at the highest densities so far achieved, will be given elsewhere.[12]

At the highest densities obtained thus far, the energy confinement properties of these discharges are comparable with calculations based on neoclassical theory. Table I provides a comparison of a representative discharge with results obtained from a one-dismensional radial transport code.[13] Briefly, the code includes contributions to the particle and heat transport from each of the the three regimes of neoclassical theory; in addition, the particle diffusion and electron heat conduction include anomalous contributions assuming transport due to current-driven drift waves. At the densities of interest here, the neoclassical coefficients dominate over $r \leq 0.9a$. The toroidal field, average density, and total current are prescribed, and the code determines the steady-state profiles. The calculated electron temperature profiles are somewhat broader than those observed; this results in larger values of q_0 than indicated by the experimental data. The numerical calculations show that the transport is appropriate to the transition region between the plateau and the Pfirsch-Schlüter regimes of neoclassical theory.

We gratefully acknowledge M. Pickrell for technical assistance, J. West for computational work, J. Terry and K. Chen for impurity measurements, and J. Rice for the soft-x-ray measurements. In addition we wish to acknowledge the contributions of the dedicated Alcator operating crew, especially S. Calogerro, C. Park, and F. Silva. We also thank Professor B. Coppi for his interest in this work. This work was supported by the U. S. Energy Research and Development Administration.

---

[a] Permanent address: United Kingdom Atomic Energy Agency, Culham Laboratory, Abingdon, U. K.

[1] G. L. Boxman *et al.* in *Proceedings of the Seventh European Conference on Controlled Fusion and Plasma Physics, Lausanne, 1975* (International Atomic Energy Agency, Vienna, 1976), Vol. 2, p. 14; ORMAK Group, in *Proceedings of the Seventh European Conference on Controlled Fusion and Plasma Physics, Lausanne, 1975* (International Atomic Energy Agency, Vienna, 1976), Vol. 2, p. 24.

[2] L. A. Berry *et al.*, in *Proceedings of the Fifth International Conference on Plasma Physics and Controlled Nuclear Fusion Research, Tokyo, Japan, 1974* (International Atomic Energy Agency, Vienna, Austria, 1975), Vol. 1, p. 101.

[3] In Ref. 2 the scaling law $\beta_\theta \sim n/I$ was given which is nearly equivalent to the scaling law of $\tau_E \sim n$.

[4] E. Apgar *et al.*, in *Proceedings of the Sixth International Conference on Plasma Physics and Controlled Nuclear Fusion Research, Berchtesgaden, West Germany, 1976* (International Atomic Energy Agency, Vienna, 1977), Vol. 1, p. 247; L. A. Berry *et al.*, in *Proceedings of the Sixth International Conference on Plasma Physics and Controlled Nuclear Fusion Research, Berchtesgaden, West Germany, 1976* (International Atomic Energy Agency, Vienna, 1977), Vol. 1, p. 46.

[5] M. Murakami, J. D. Callen, and L. A. Berry, Nucl. Fusion 16, 397 (1976).

[6] S. M. Wolfe *et al.*, Appl. Opt. 15, 2645 (1976).

[7]B. Basu *et al.*, in *Proceedings of the Sixth International Conference on Plasma Physics and Controlled Nuclear Fusion Research, Berchtesgaden, West Germany, 1976* (International Atomic Energy Agency, Vienna, 1977), Vol. 2, p. 455.
[8]K. Molvig, Bull. Am. Phys. Soc. 21, 1125 (1976).
[9]M. H. Hughes *et al.*, to be published.
[10]J. E. Rice and H. I. Helava, Bull. Am. Phys. Soc. 21, 1141 (1976).
[11]J. L. Terry *et al.*, John Hopkins University, Technical Report No. COO-2711-3, 1977 (unpublished).
[12]A. Gondhalekar, D. Overskei, R. R. Parker, and J. West, to be published.
[13]M. H. Hughes and D. E. Post, Princeton Plasma Physics Laboratory Report No. 1335, 1977 (to be published).

Observation of Severe Heat-Flux Limitation and Ion-Acoustic Turbulence in a Laser-Heated Plasma

D. R. Gray, J. D. Kilkenny, and M. S. White
Blackett Laboratory, Imperial College, London, United Kingdom

and

P. Blyth and D. Hull
Atomic Weapons Research Establishment, Aldermaston, United Kingdom

(Received 12 September 1977)

The thermal conductivity of a plasma of density 6×10^{16} cm^{-3} is measured when it is heated by a 300-MW, 3-ns CO_2 laser pulse. The data are best represented using a heat flux which is limited to $\sim 4\%$ of the free-streaming limit. Low-frequency turbulence is observed of sufficient intensity to cause this flux limit.

In this Letter we report definitive measurements of the thermal conductivity of a laser-heated plasma when the temperature gradient is large and an ion-acoustic instability is excited. The classical treatment of thermal conductivity[1] has been by a first-order perturbation to a Maxwellian. However, when λ_e/L (the ratio of the electron mean free path to the temperature-gradient scale length) is greater than 0.02, second-order terms dominate and there seems to be no rigorous theory. Here we use

$$\lambda_e/L = 2.292\times10^{13}T_e\,|\nabla T_e|\,n_e\ln\Lambda, \qquad (1)$$

with T_e in eV and n_e in inverse cubic centimeters. We have previously measured the thermal conductivity[2] with $T_e = T_i$ and $\lambda_e/L \sim 0.04$ and found a reduction by a factor of 2 from Spitzer's value. When $T_e \gg T_i$, the return current from the heat flow can drive an ion-acoustic instability, which would decrease the heat flux.[3,4] Here we have increased λ_e/L to 0.5 (from Ref. 2) and with $T_e \sim 5T_i$ have seen a very low thermal conductivity accompanied by low-frequency turbulence.

As before, our measurement is based on ruby-laser light scattering. We have extended this technique to spatial and temporal resolutions of 200 μm and 1 ns. Other experiments on laser-produced plasmas[5-7] have used much less direct diagnostics to measure thermal conductivity. Many other phenomena (magnetic-field generation, resonant absorption, atomic physics, fast-electron transport) complicate these experiments. In contrast, our experiment has to our knowledge none of these extraneous phenomena.

The plasma used has been described previously.[2] It was a weak hydrogen Z pinch with initial density and temperature of 6×10^{16} cm^{-3} and 4 eV, respectively. The center of this plasma was heated by a 300-MW, 3-ns CO_2 laser pulse, focused to a measured spot size of 350 ± 50 μm. Ruby-laser light scattering at 90° was performed with the differential scattering vector ($\vec{k}_s$) both parallel and perpendicular to ∇T_e. The scattering parameter α was in the range $0.5<\alpha<1.5$. The electron density and temperature were obtained by fitting shifted Salpeter curves for different α's to the electron features. This method is described by Kunze.[8] The error bars on density and temperatrue were determined by the range of the values of α which would fit within the experimental error bars. These values of n_e agreed with those obtained using a Rayleigh calibration of the system. A fast photomultiplier (RCA C31024A) gave a 1.2-ns time resolution. Reproducibility was good enough to plot spectra on a shot-to-shot basis. The spatial resolution